RESEARCH

Electrospun Polysulfone Hybrid Nanocomposite Fibers as Membrane for Separating Oil/Water Emulsion

Deepalekshmi Ponnamma[1] · Yara Elgawady[2] · Mohamed K. Hassan[2] · Samer Adham[3] · Mashael Al-Maas[3] · Karim Alamgir[4] · Mariam Al Ali Al-Maadeed[1,2]

Abstract

Commercial polymer membranes are largely utilized to separate oil/water mixtures; however, membrane fouling, flux decline, and short lifetime often inhibit their high performance. In order to resolve these drawbacks of the commercial membranes, we introduce a surface modification strategy following the electrospinning method. Electrospun fibers of polysulfone (PSf)/ iron oxide (FeO)/halloysite nanotubes (HNT) nanocomposite are applied to modify the polyether sulfone (PES) standard membrane support surface for developing highly efficient oil/water emulsion separating membranes. This facile and simple spinning process for shorter periods ensures nanocomposite coatings on the standard PES membranes and allows a better oil/water separation. We analyze the structural and morphological characteristics of the modified membrane surface using scanning electron microscopy, Fourier transformation infrared spectroscopy, and X-ray diffraction studies and hydrophilicity from contact angle studies. FeO nanoparticles of 2–5 nm and HNTs of < 50 nm size mixed in PSf produce fibers of 531 ± 162 nm average diameter at a relatively lower applied electrical voltage of 14.5 kV, compared to PSf. Underwater and under-oil contact angle values are used to prove the surface characteristics of the membranes and total organic content (TOC) values for the emulsion separation performance. From PES support to PSf and PSf/HNT-FeO, the TOC values respectively change from 67 to 75 and 79%. We find moderately hydrophilic membranes (PSf/HNT-FeO) resulting in a higher permeate flux (28,447 $Lm^{-2} \cdot h^{-1}$) and quicker separation performance. We believe this study provides a notable solution to modify the surface of commercial membranes for better emulsion separation performance.

Keywords Hydrophilicity · Emulsion · Fibers · Nanocomposites · Water purification

Introduction

Membrane-based separation technology is one of the most promising oil/water separation methods due to its low energy requirement, high efficiency, reusability for successive cycles, and environmental protection [1–3]. Ultrafiltration and microfiltration technology are popular separation methods; however, surface adsorption of oils and blockage of pores cause declined filtration performance [3]. Secondary separation techniques are also used with the current procedures since single treatment methods are insufficient to fulfil the quality standards for filtered water [4]. Nanofiltration is a possible and effective method used for primary and secondary separation [5]. Major limitations of oil-water separating membranes include long-term stability and fouling resistance, which are improved by suitably modifying the materials used for membrane fabrication. Industries use pressure-driven membranes for oil-water separation, and fouling is one of the major disadvantages of such processes [6, 7]. In addition, cleaning the used membranes by squeezing out the oil blocks the membrane pores, decreasing separation efficiency over a long time [8]. Gravity-driven separation or separation under low pressure is a possible solution to this kind of issue [9, 10].

✉ Deepalekshmi Ponnamma
  deepalekshmi@qu.edu.qa

1   Materials Science and Technology Program, Department of Mathematics, Statistics and Physics, College of Arts and Sciences, Qatar University, 2713 Doha, Qatar

2   Center for Advanced Materials, Qatar University, P. O. Box 2713, Doha, Qatar

3   ConocoPhilips Global Water Sustainability Center, Qatar Science and Technology Park, Doha, Qatar

4   Department of Chemical & Biomolecular Engineering, University of Houston, S222 Engineering Bldg 1, 4726 Calhoun Rd, Houston, TX 77204, USA

Polymers are widely applied in fabricating separation membranes. Numerous inorganic nanomaterials with high aspect ratio, tunable pore size, high chemical and thermal stability, and unique surface chemistry are introduced into the polymer medium to generate advanced composite membranes [11–13]. These membranes report excellent antifouling properties, good permeation, recyclability, and thermomechanical stability [14, 15].

Electrospinning is a promising strategy for nanocomposite fabrication, and Su et al. recently reviewed advanced nanofibrous membranes for oil-water separation by electrospinning [16]. The interconnected pore structure and possible tuning of nanofiber diameter are mainly responsible for the enhanced oil/water separation efficiency of the electrospun fibers [17]. Based on the surface properties, the current oil/water separation electrospun membranes can be superhydrophobic, super hydrophilic, or intelligent membranes with external stimuli response wettability [16]. While hydrophobic membranes allow free permeation or absorption of oil molecules, hydrophilic membranes reject oil droplets and allow only water molecules to pass through. Recent studies from our group report multiple hydrophobic membranes from electrospun nanocomposites containing nanoparticles of mesoporous silica [18], carbon nanotubes [19], cobalt oxide [20] etc., with good oil absorption performances. In all cases, the composites exhibited good oleophilic properties and thus helped much in higher rates of oil absorption performance. It is established that the superhydrophobic membranes are suitable for removing oil from water in oil emulsions, whereas the superhydrophilic membranes help treat oil in water emulsions [16]. However, developing membranes by properly balancing the separation efficiency and permeation flux remains challenging due to the high porosity and pore size for the electrospun fibers. Moreover, the simultaneous enhancement is water flux and purity of obtained water after filtration is another significant challenge to resolve [21].

Recent studies about the electrospun fibers for oil-water emulsions reveal interesting structural and functional properties. Superhydrophilic and underwater superoleophobic fibers of polyvinylidene fluoride (PVDF) were fabricated by coating with graphene oxide (GO)-chitosan nanostructures for wettability modification [22]. The measured average flux was $31{,}673 \pm 1447$ $Lm^{-2} \cdot h^{-1} bar^{-1}$ under 0.4 bar pressure difference with 99% separation efficiency. Similar studies such as GO stabilized triptycene poly(ether ether sulfone)-CH_2NH_2:HCl polymer membrane [23], zwitterion PVDF-imprinted composite membrane [24], and stalactite-shaped TiO_2-SiO_2 composite nanoparticles modified multilayer fiber glass superhydrophobic membrane [25] report excellent emulsion separation ability with photocatalytic activity, antibacterial activity etc. as the additional characteristics. Halloysite nanotubes (HNT) are used to modify

polydopamine-Mxene composite, and the resulting membrane rejected petroleum ether and lubricating oil by 99.8% [26]. Hydrophilicity, formation of stable dispersions, high biocompatibility, and great adsorption capacity are notable features of HNTs, and therefore, they are widely used for water purification.

Polysulfone (PSf) is a suitable polymer for fabricating separation membranes [27], and it is blended with different polymers like polyether sulfone (PES), polyethylene glycol, and polyetherimide, to improve the membrane performance and reduce the fouling effect [28]. Obaid et al. developed superoleophobic PSf membranes by immersing electrospun polymer fibers in NaOH solution of different concentrations at various temperatures and times [8]. The optimized membrane effectively separated soyabean oil and hexane water mixtures with respective fluxes of 11,865 and 14,016 LMH even after the 5th cycle of gravity driven separation. The efficiency obtained was 99.99% with 1–3 ppm oil concentration in the filtrate. Surface modification of PES is reported by introducing TiO_2 nanoparticles [29], blending with polyvinyl alcohol (PVA) and polyamide imide [30]. Cheshomi et al. designed new thin film composite membrane from Pebax coated PES-PSf blend and later by incorporating TiO_2 nanoparticles by dip coating [31]. When the TiO_2 concentrations were respectively 0.03 and 0.01 wt%, maximum permeate flux of 75.32 and 46.32 $Lm^{-2} \cdot h^{-1}$ along with humic acid rejection rates of 98.22 and 99.14% were achieved.

In this paper, we report a facile and easy surface modification technique on the PES support by electrospinning the PSf nanocomposites containing hydrophilic nanoparticles of FeO and HNT. The combined morphology of the nanomaterials and their incorporation in the PSf will strengthen the interfacial interaction and provide sufficient attachment with the PES support. The surface modification of the commercial polymer membrane with electrospinning in a limited time is significant in simple, less energy manufacturing. Outstanding oil-water separation efficiency is achieved due to the controlled hydrophilicity of the membranes. The hybrid or synergistic influence of the nanomaterials and the superior dispersion rate of the nanoparticles in PSf, ensured by the solution mixing, ratify nanomaterial networks within the electrospun fibers. The surface properties and contact angle values of the nanocomposite membranes disclose the controlled oil/water interaction ability, thereby contributing to the outstanding emulsion separation performance.

Experimental Section

Materials

Iron (III) acetylacetonate ($\geq 99.9\%$ pure) with M_W: 353.17 g/mol, N, N-Dimethylformamide (Anhydrous 99.8%) with

M_W: 73.09 g/mol and HNT with M_W: 294.19 g/mol were purchased from Sigma–Aldrich. The polymer polysulfone (PSf) pellets were also obtained from Sigma–Aldrich. The polyether sulfone (PES) support with 0.2 μm pore size was commercially obtained from Sterlitech Corporation.

Synthesis of Nanomaterials

While iron oxide (FeO) is synthesized by reflux reaction, HNT is used as a template for the in situ growth of the FeO. In order to prepare the DMF-stabilized iron oxide nanoparticles, a solution of $Fe(C_5H_7O_2)_3$ (iron acetyl acetonate) in DMF was prepared (0.1 M, 0.5 ml) in 50 ml DMF and then injected into a round bottom flask fitted to a reflux system. The reflux reaction was done for 8 h by heating the mixture at 140 ℃ in an air-open atmosphere. A perfectly dispersed reddish solution of iron nanoparticles was observed by the end of the chemical reaction [32]. In the same way, the reflux reaction was continued in the presence of 0.1 g HNT dispersed in 50 ml DMF solution to obtain the FeO-HNT hybrid filler system. The reaction conditions were also mimicked for HNTs alone (refluxing 0.1 g HNT in 50 ml DMF) without doing any FeO synthesis in situ. Thus, three nanoparticles, FeO, FeO-HNT, and HNT, were analyzed and utilized for manufacturing the composites.

Fabrication of Polymer Nanocomposite Membranes

Neat PSf pellets in 25 wt% were dissolved in DMF (2.5 g in 10 ml) by overnight magnetic stirring at room temperature. Similarly, the PSf pellets (2.5 g) were dissolved in FeO suspended DMF (10 ml suspension) and FeO/HNT suspended DMF (10 ml suspension) in 25 wt% by magnetic stirring overnight to respectively fabricate the PSf/FeO and PSf/FeO-HNT nanocomposite dispersions. HNT composite was also generated similarly by dissolving 2.5 g PSf in 10 ml HNT suspension in DMF after reflux. In all cases, overnight magnetic stirring was practised, and the stable suspensions of the polymer nanocomposites were electrospun using the following feed rate and applied voltage (Table 1) on a PES substrate of 0.2 μ pore size. The electrospinning process was done at room temperature, and all the electrospun nanofibers were collected on the PES by keeping the distance between

Table 1 Sample details and electrospinning conditions

Sample	Feed rate (ml/h)	Voltage (KV)
Neat PSF	1 ml/h	18
PSF-HNT	1 ml/h	20
PSF-FeO	1.5 ml/h	16.7
PSF-HNT/FeO	0.6 ml/h	15.5

the tip of the spraying needle and the collecting stage at 9 ± 1 cm.

Characterization Techniques

Morphology studies of the nanomaterials FeO, HNT, and FeO-HNT were done by transmission electron microscope (TECNAI G2 TEM, TF20 model), and that of the electrospun fibers were done by scanning electron microscope (Nova Nano SEM 450) with a voltage variation from 200 V to 30 kV. All samples were gold sputtered before analyzing the SEM morphology. The average fiber diameter for the electrospun composite fibers was calculated using the ImageJ software. Structural properties of the nanomaterials and nanocomposite fibers were identified using Energy dispersive spectroscopy (equipped with SEM), X-ray diffractometer (XRD, PANalytical Empyrean diffractometer, with Cu Kα radiation of 1.54 nm wavelength), and the Fourier transformation infrared spectroscopy (Thermo Nicolet/FTIR 670). While the XRD scans the materials from 10 to 90° at a scan step size of 0.013° per minute, the FTIR spectrum was recorded from 400 to 4000 cm^{-1} at 2 cm^{-1} per minute. The mechanical stability of the fibers was tested using the universal testing machine and the 2 cm $\times$ 5 cm $\times$ 0.7 mm rectangular pieces. Surface wettability of the PSf composite modified PES support samples was monitored by the oil and water contact angle measurements according to the sessile drop method, using a Data physics contact angle goniometer (fitted with OCA35 system and CCD camera). The contact angle was measured using the Young-Laplace model directly correlated to the surface roughness. Both oil and water droplets of 3 μL volume were placed atop the fibers, and a grace period of 3 s time was given before a contact angle measurement. Testing was repeated five times, focusing on different parts of the sample. Underwater and under-oil contact angles were tested using separate needle set up for correct angle measurements. Oil/water separation efficiency of the membrane was also tested using the simple oil/water mixture (2 ml mineral oil of density 0.87 g/ml and viscosity 154 mPas, in 10 ml water) and oil in water emulsion. The preparation of the emulsion was done by the following method: an oil/water emulsion was made at 200 ppm oil concentration and by dissolving 0.14 wt% of SDS (sodium dodecyl sulfate) in the mixture by ultrasonication for 2 h [33]. The size of the oil droplets in the stable suspension was determined to be 2–3 μm using the NMR spectroscope.

UF Bench-Scale Setup and Testing Protocol

UF bench-scale tests using an Amicon stirred cell (Millipore, USA) were conducted following an experimental protocol developed in previous studies [14]. Initially, the protocol involves testing the clean membrane using deionized (DI)

water at a pressure of 0.5 bar and stirring speed of 560 rpm until obtaining stable water flux measurement. The membrane was then tested using synthetically produced water (PW) prepared using crude oil (containing approximately 75% saturated alkanes and 25% aromatic hydrocarbons) with a pH ~ 6. For organic rejection, permeate samples were collected for total organic carbon (TOC) analyses using a TOC Analyzer (TOC-V, Shimadzu, Japan). Membrane fouling was then assessed by performing a second DI water test (i.e., final baseline) at similar operating conditions. Finally, chemical cleaning consisted of sodium hydroxide (~ 1 mM NaOH and pH of ~ 11.5 at ~ 25 °C), sodium dodecyl sulfate (~ 10 mM solution and pH of ~ 9.4 at 35 °C), and another DI water baseline to determine the final membrane flux. After each cleaning cycle, the pH was adjusted to ~ 7 by immersing in distilled water and washing thereafter.

Results and Discussion

Morphology and Structural Analysis of the FeO, HNT and FeO/HNT

The three nanomaterials stabilized in DMF (FeO, HNT, and FeO/HNT) were analyzed to know their morphological and structural features. Figure 1 illustrates the TEM images and the EDS elemental analysis for all samples. The TEM image for FeO (Fig. 1a) clearly shows the very small particle size of the nanomaterials, typically in the range of 2–5 nm [32]. The nanoparticles are in spherical forms with less agglomeration, indicating the well-stable DMF suspension [34]. For the HNT, the average diameter is ˂ 50 nm, as represented in Fig. 1b. The hybrid suspension of FeO/HNT shows a mixture of both nanomaterials by maintaining their structural integrity as expected.

The EDS elemental analysis results for all samples indicate the presence of particular elements in the suspension without the presence of any foreign materials. This clearly illustrates the phase purity of the synthesized nanomaterials. In the DMF stabilized FeO suspension, the Fe^{2+} ionic species are chemically bonded to DMF through coordination bonds, which is responsible for the high stability of the nanomaterial [32].

XRD diffraction pattern for the nanomaterials is good evidence for their structural properties. Figure 2 shows the XRD pattern obtained for all nanomaterials FeO, HNT, and FeO/HNT compared to the glass substrate used to coat the dispersed nanomaterials in DMF. As expected, the blank glass substrate shows a uniform flat curve. The FeO nanomaterials show different peaks at 10.7, 13.0, 16.8, 21.5,
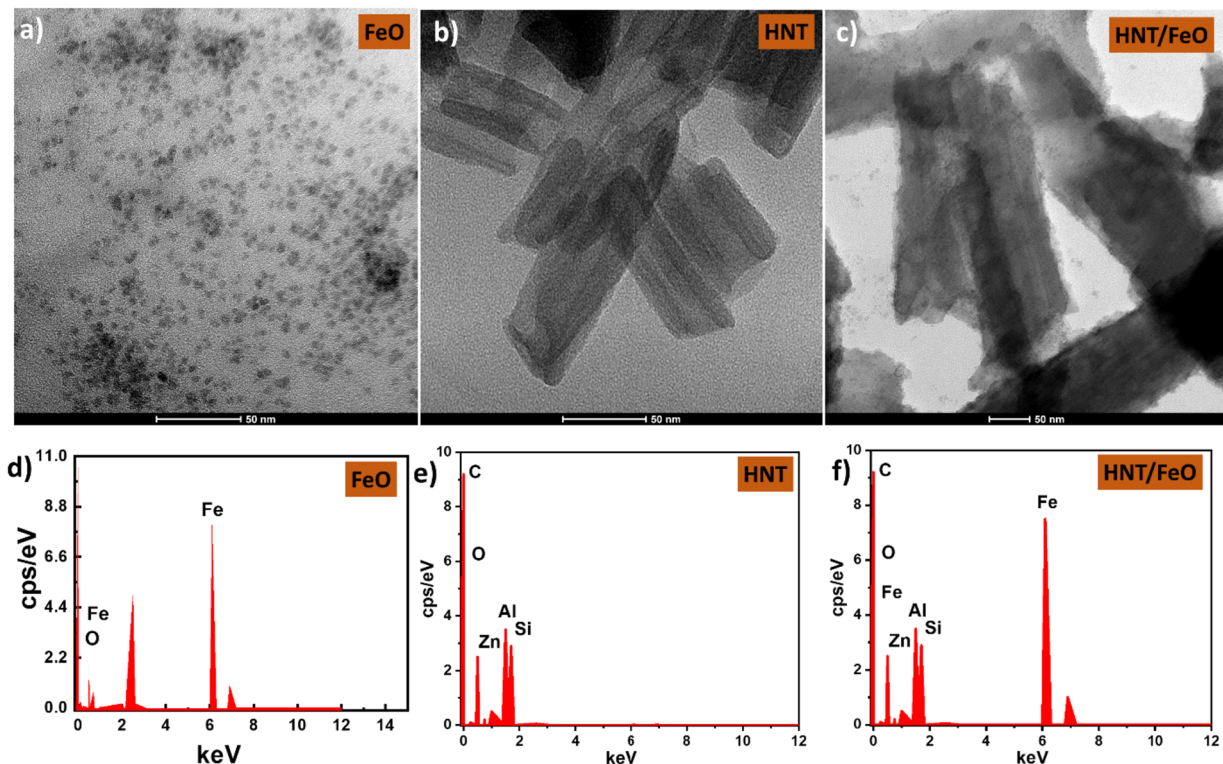

Fig. 1 Transmission electron microscopic images of FeO (**a**), HNT (**b**), and FeO/HNT (**c**) nanomaterials, with EDS spectra FeO (**d**), HNT (**e**), and FeO/HNT (**f**)
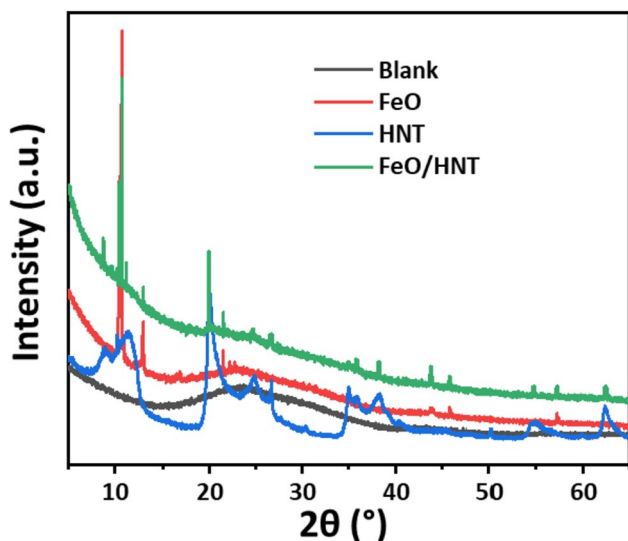
Fig. 2 XRD pattern for the synthesized nanomaterials: FeO, HNT, and FeO/HNT compared to the dispersed glass substrate

43.7, and 57.2° corresponding respectively to the crystalline planes of (111), (012), (104), (220), (400), and (511) [35]. For HNT, the diffraction peaks appear at 11.3, 19.9, and 24.7°, respectively, related to the (001), (020), and (002) crystalline planes [36]. However, for the nanohybrid material FeO/HNT, the pattern shows a hybrid or combined effect of the two nanomaterials FeO and HNT, which indicates the structural integrity and stability of both nanomaterials.

Morphology and Structural Analysis of the PSf Composites

Figure 3 shows the SEM images of the PSf and its composite fibers with the corresponding fiber diameter histograms. The smaller variations are observed for the fiber appearance, and the diameter as the nanomaterials are introduced into the PSf medium. Depending on the concentration of the polymer solution and the applied voltage, the Taylor cone regions of the nanocomposite solution fluctuate and thus cause mass flow variation to the downstream jet. This eventually causes variations in the charge distribution on the jet surface, thus attributing to the fiber diameter changes. When the applied voltage is varied, an imbalance is created between the solution supply to the needle tip and its electric field-assisted withdrawal [37]. As per Table 1, the applied voltage required for the neat PSf is 18 kV, and it reduces when the composites with FeO and HNT systems are electrospun. It is established that, at higher applied voltages, the Taylor cone becomes more tapered and finally disappears beyond a particular voltage value. At this stage, the jet originates directly from the nozzle tip. In other words, a higher voltage enhances the rate of solution removal from the Taylor cone, which exceeds the solution delivery rate

to the tip [38]. When PSf-FeO/HNT hybrid nanocomposite is compared with the neat PSf, the average fiber diameter changes from 531 ± 162 to 259 ± 107 nm, with the respectively applied voltage varying from 14.5 to 18 kV. At higher voltages, the Taylor cone can also split into multiple jets and thus can cause a lower diameter [39]. Since the fiber diameter increases with the introduction of FeO and HNT nanomaterials, especially for the hybrid nanocomposite containing 1 wt% of FeO/HNT, the mechanical rigidity will be the highest. This helps the nanofiber withstand the water flux while conducting oil/water separation studies. The EDS mapping image shown in the Fig. 3d inset demonstrates the uniform distribution of all elements present in the nanoparticles on the surface of fibers.

Figure 4 demonstrates the structural properties of the PSf nanocomposites through the FTIR and XRD studies. The peaks at 1244 cm^{-1}, 1489 cm^{-1}, and 1585 cm^{-1} in the FTIR spectrum are typical absorption bands for PSf [40]. The main characteristic absorption band (1152–1160 cm^{-1}) comes from (SO_2) of sulfone groups (symmetric stretching of sulfone ($C-SO_2-C$)), usually fragmented into band groups as obvious in the spectrum [41]. Asymmetric stretching ($C-SO_2-C$) at 1319 and 1292 cm^{-1} is also observed. The graph also shows the solid reflectance of benzene ring stretching approach at 1583−1502 cm^{-1}. Strong vibrations in the spectra at 831, 850, and 871 cm^{-1} are due to aromatic C-H bending [42]. The band during 579–635 cm^{-1} can correspond to the vibration of the Fe-O bonds. The characteristic absorption peaks of the pristine HNT, such as the O-H stretching of inner hydroxyl groups at 3625 cm^{-1}, O-H deformation of water at 1631 cm^{-1}, O-H bending of inner hydroxyl groups at 906 cm^{-1}, and Si-O stretching at 1004 cm^{-1} [43, 44].

XRD analysis further demonstrates the structural properties of the PSf composites (Fig. 4c). For PSf, a wide and weak diffraction peak is located at 2θ value of 17°, attributed to its amorphous structure. All composites containing nanomaterials such as FeO, HNT, and FeO/HNT show a similar XRD pattern as pure PSf, with slight broadening for the HNT-containing composites. The less broadening for PSf-FeO can be attributed to the structural property of the FeO nanoparticles and its crystalline nature. However, the HNT and FeO/HNT cause increased disorder in the polymer chains and, thus, highly amorphous nature. The lack of the diffraction peaks related to the nanoparticles can be due to the well dispersion of FeO, HNT, and FeO/HNT (1 wt% each) in the PSf polymer matrix [45].

Surface Wettability Behavior of PSf Composite Membranes

The oil/water separation performance of a membrane depends on the surface wettability and contact angle values. The wettability again depends on the chemical
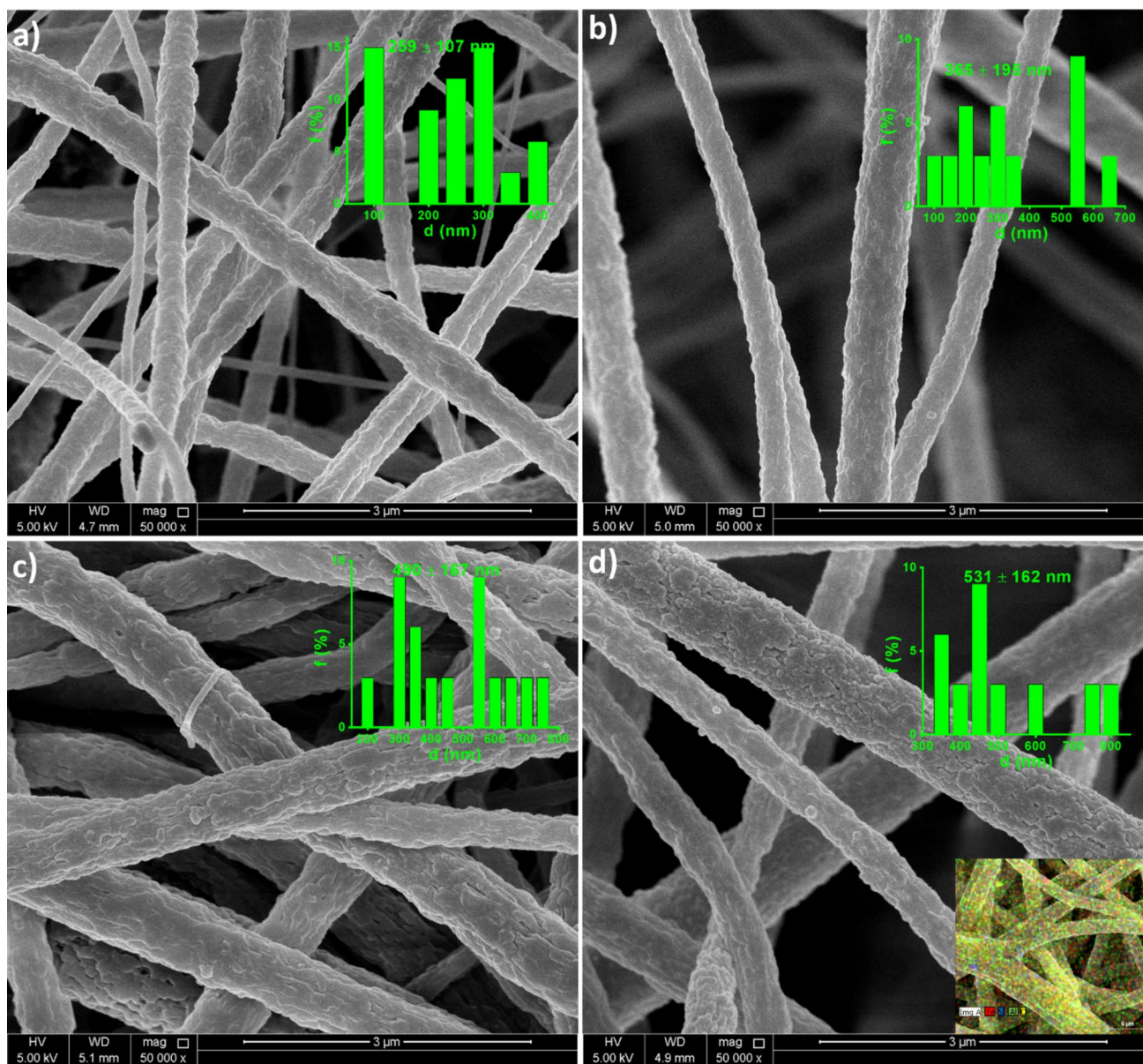
Fig. 3 SEM images and the corresponding fiber distribution histograms for Neat PSf (**a**), PSf-FeO (**b**), PSf-HNT (**c**), and PSf-FeO/HNT (**d**) nanocomposite fibers, inset of EDS mapping image for the PSf-FeO/HNT sample (**d**)

composition and roughness features of the membrane surface. Studies also prove the high-level distribution and low surface energy of nanoparticles influencing the hydrophobicity and, thus, the oil-water separation [46, 47]. Wenzel model states that the hydrophilic membrane becomes more hydrophilic, and an oleophilic membrane becomes more oleophilic due to their increase in surface roughness due to the capillary effect [48]. The water and oil contact angles for the PSf nanocomposite membranes are demonstrated in Fig. 5. When the PES support is exposed to water and oil droplets, the contact angle values were respectively 123.18 ± 2.54 and 29.96 ± 2.36. In the case

of oil droplet, it spreads out quickly on the surface, proving the comparatively higher oleophilicity/hydrophobicity of the membrane. However, modification of the PES substrate with PSf and its composite containing HNT and FeO hybrid particles, the contact angle values change (Fig. 5a). It is observed that the hydrophobicity is the maximum for the neat PSf-coated membrane, and the water contact angle reduces with the introduction of the nanomaterials to PSf. At the same time, the oil contact angle does not show a huge variation, and the hybrid composite containing FeO/HNT at 1 wt% maintains moderate oleophilicity and hydrophobicity so that this sample is capable of

Fig. 4 FTIR spectra (**a**, **b**) and XRD pattern (**c**) for the PSf and its nanocomposites
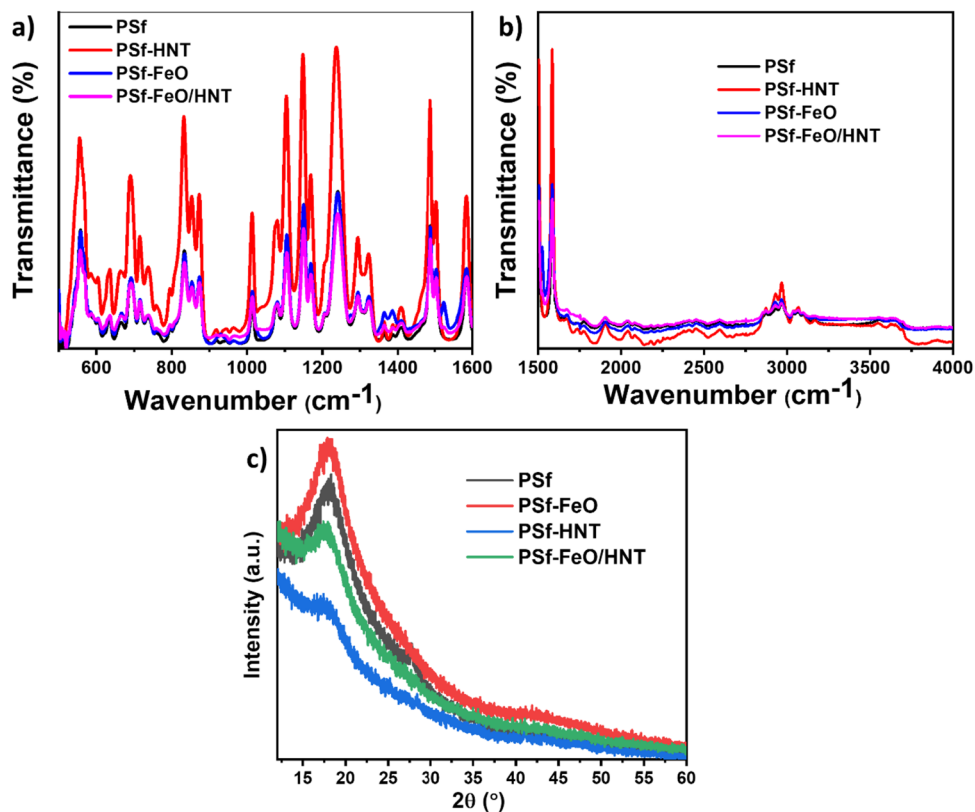
separating oil molecules from a typical oil/water mixture than absorbing it.

Figure 5b and c, respectively, shows the underwater oil contact angle and the under-oil water contact angle for the hybrid nanocomposite (PSf-FeO/HNT) modified membrane. On immersing the nanocomposite modified PES support membranes in to water or oil medium, the air in the surface is occupied by a continuous phase. When the oil/water droplets are introduced to check the underwater contact angle for oil and under oil contact angle for water, the gas (trapped air)-liquid (immersed medium)-solid (membrane) three-phase interface is converted to liquid (introduced droplet)-liquid-solid interphase achieving the underwater oleophilicity or under oil hydrophobicity [49]. In addition, the adhesion property of the membrane towards oil/water is also clear from the contact angle studies. The PSf-FeO/HNT shows good hydrophobicity when immersed in oil and oleophilicity when immersed in water. It is evidenced by the flat shape of the underwater oil droplet and by the quasi-spherical shape of the under-oil water droplet [48]. This is attributed to the unique wetting characteristic due to the surface modification (electrospinning) process done on the PES support.

Though the membrane is oleophilic the contact angle values do not fall to 0°, which is a good indication of good separation ability of the membrane. In other words, rather than fully absorbing the oil molecules, the membrane will be capable of separating the water and oil from a given mixture of oil/water emulsion. While introducing the water droplets to membrane surface in oil, the trapped oil molecules in the microstructure decreases the water-membrane contact area and enhances the water contact angle [50]. At the same time, in water medium, the trapped water molecules prevent the oil from their direct contact to the membrane. This behavior of the membrane is a good indication of their application in oil water separation.

Separation of Oil/Water Emulsion by the PSf Nanocomposite Membrane

UF Bench-Scale Testing Results

The performance of the modified PES membranes, specifically ones with PSf, PSf-HNT, PSf-FeO, and PSf-FeO/HNT nanocomposite materials, are compared against the neat PES membrane (i.e. commercial support) through UF testing. Figure 6 presents the experimental flux results normalized by the applied pressure in $L/m^2.h.bar$ (LMH/bar) obtained for the tested membranes. The figure shows that the applied modifications on the PES membrane did not significantly impact the membrane's initial water permeability. Although a drop in membrane flux was observed after testing the modified membranes with the synthetic PW, it did not cause membrane fouling, which was confirmed through the final DI water baseline

Fig. 5 a Water and oil contact angles for the PSf and its nanocomposite coated PES substrate in air; under water oil contact angle (**b**) and under oil water contact angle for the PSf-FeO/HNT nanocomposite coated PES membrane (**c**)
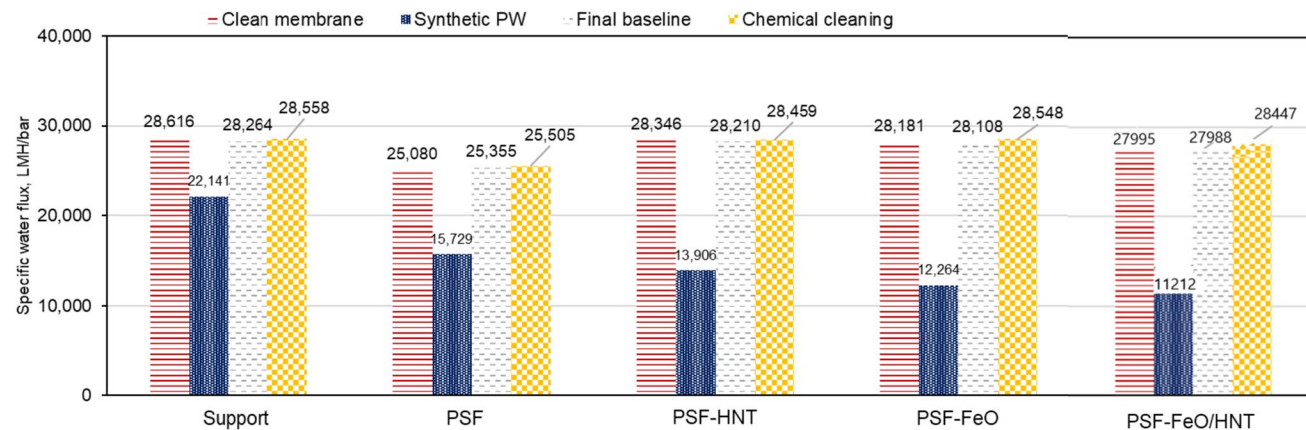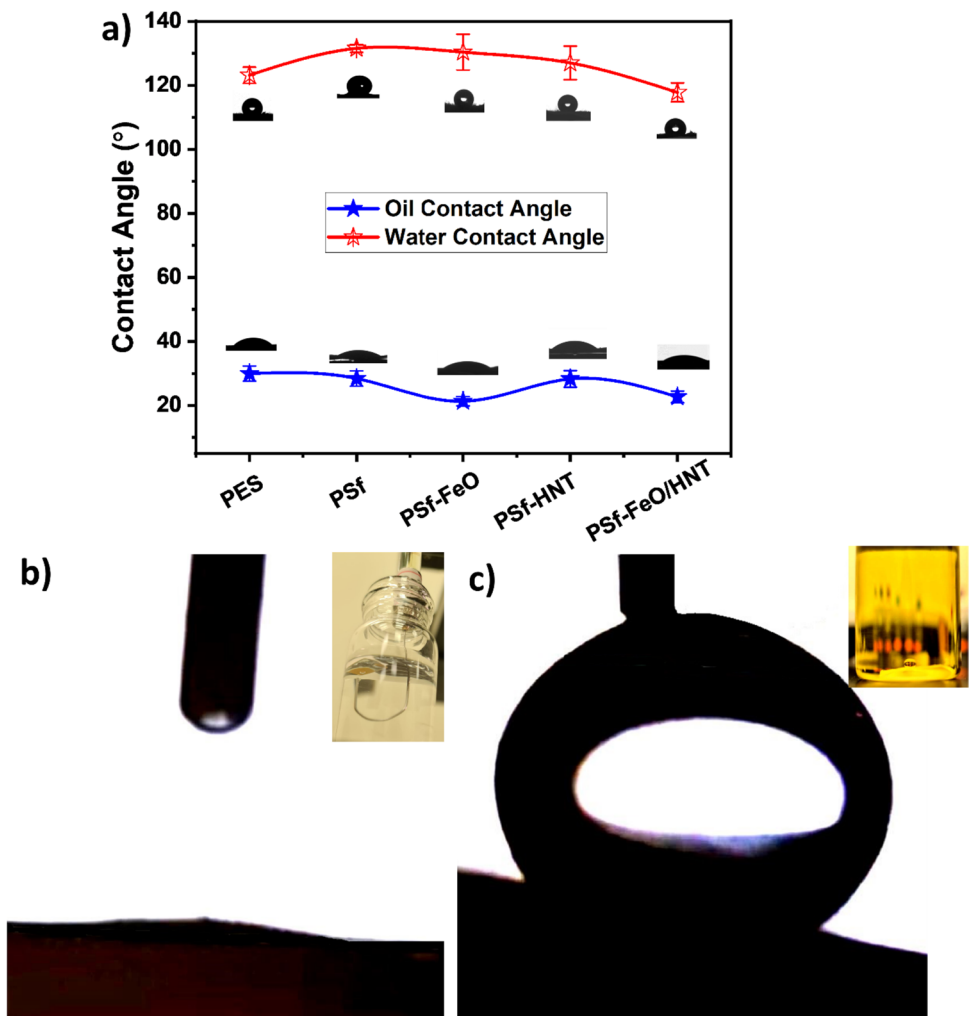

Fig. 6 UF bench-scale testing results on PES modified membranes

[51, 52]. The TOC rejection of the neat PES membrane was improved after applying the PSF nanocomposite from 67 to 75%, as indicated in Table 2. The addition of HNT/FeO significantly improves the TOC rejection. The stability of the membrane is also according to the reported data [52], by which the membranes start to deteriorate after three cycles.

Table 2 UF bench-scale testing results—organic rejection performance

PES support	Feed TOC mg/L	Permeate TOC mg/L	TOC rejection %
Neat	27	8.1	67
PSf		6.8	75
PSf-HNT		6.7	75
PSf-FeO		6.2	77
PSf-FeO/HNT		5.9	79

Fig. 7 Separation process for the oil/water mixture and the oil/water surfactant stabilized emulsion by the PSf-FeO/HNT nanocomposite modified PES support membrane by gravity driven separation process

Gravity Filtration Screening Tests

Gravity-driven filtration screening tests on the PSf-FeO/HNT membrane were also performed using a normal oil/water mixture and a surfactant stabilized oil in water emulsion to test the efficiency of the membrane in separating oil/water mixtures. Figure 7 represents the images obtained during the oil/water separation process. In order to test the oil/water separation in the first case, a mixture of engine oil in colored water (mixed with Azocarmine G dye) was used, as shown in the figure. The gravity separation for about 4 h separated about 8 ml of water with a separation efficiency of 2 ml/h. The second experiment in the figure demonstrates the separation of

oil/water surfactant stabilized emulsion. Since the density of water is higher in the oil/water emulsion, the membrane was pre-wetted with water to make it oleophobic in water to separate the water [53] selectively. Figure 7 shows the oil-water separation process for the PSf-HNT/FeO modified PES membrane. When the oil/water emulsion is passed through the membrane, the water passes through it, leaving the oil behind. The permeated water is much more transparent when compared to the oil/water emulsion, and the permeate and the feed are analyzed for their total organic content values. During the emulsion separation, the oil molecules combined with the surfactant ions has a tendency to aggregate due to electrostatic repulsive interaction (anionic surfactant and charged oil in water droplets). This helps in the migration of oil/surfactant ions leaving the water molecules and finally causing the separation. Unlike the standard procedure of oil/water separation using vertical injection of the feed [9, 10, 54], the simplicity and easiness of the separation are proved here, by following the syringe injection. This method ensures the easily applicable nature of the membranes for emulsion separation.

When the TOC test results were compared, the PSf-FeO/HNT modified PES support membrane was observed to be capable of reducing the TOC value of the oil/water emulsion from 90.545 to 43.625 ppm in the first cycle of the experiment. These feed and permeate emulsions were also tested for the droplet size using the NMR studies, and the average droplet size respectively varied from 2 to 3 µm to < 200 nm. These results evidence the capability of PSf composite modified PES in separating oil/water emulsions.

Table 3 compares the efficiency of the synthesized membrane with similar studies reported in the literature. The significance of the current study is clearer from the table.

Conclusions

Electrospun nanocomposites of PSf nanocomposites containing FeO/HNT nanomaterials were applied to modify the surface properties of the PES membrane. All modified fibers exhibited an average fiber diameter change of 531 ± 162 (PSf-FeO/HNT) nm to 259 ± 107 nm (PSf), with the increase in spinning voltage. The higher fiber diameter for the composite compared to neat polymer proved the mechanical integrity of the fibers. The nanocomposite fibers impart moderate oleophilicity, enabling the membrane to separate the oil/water emulsion efficiently. Nanocomposite fibers showed good hydrophobicity when immersed in oil and oleophilicity when immersed in water, as evidenced by the flat shape of the underwater oil droplet and the quasi-spherical shape of the underoil water droplet. UF bench-scale tests conducted on the modified membranes, namely PSf, PSf-HNT, PSf-FeO, and PSf-FeO/HNT confirm the enhancement in TOC rejection after adding the nanocomposite materials on the commercial membrane. In

Table 3 Comparison of the current study with the existing research on electrospun membranes

Nature of composite	Oil/water separation efficiency	Highlighted property	Ref:
Hydrophilic PAN//GO-SiO$_2$//PAN-SiO$_2$ triple layer membrane	$^>$97% pump oil rejection rate; 423.7 ± 7.1 L/m^2·h toluene flux	Microfiltration	[55]
Superhydrophobic CNT/PVDF membrane	9270 L m^{-2}·h^{-1} oil-water separation flux and > 99% separation efficiency under gravity	Questionable polluting effects of CNTs to filtrate	[56]
Spraying 3D TiO$_2$@crumpled graphene oxide core-shell sphere on electrospun poly (arylene ether nitrile) (PEN) porous support	3142–3514 L·m^{-2}·h^{-1} flux stable rejection rate over 99%	Particles anchored on the membrane can cause pollution	[57]
Polyphenylene sulfide spun on polyvinyl alcohol (PVA) sacrificial template/PAN supporting substrate	Maximum flux of 1707 Lm^{-2}·h^{-1} under gravity; and 99% separation efficiency	Complex preparation method	[58]
Superhydrophobic fibrous PVA and agar/PVA membrane	Water flux of 1136 Lm^{-2}·h^{-1}bar^{-1} with $\geq$ 99.9% separation efficiency	Complex preparation method	[59]
Current work of PSf/FeO-HNT modified PES substrate	28,447 Lm^{-2}·h^{-1} specific water flux with 79% oil rejection	No chance of secondary pollution due to in situ composite formation.	Current work

addition, these modified membranes showed low fouling propensity and good cleanability. Gravity screening tests applied on the PSF-FeO/HNT membrane also showed a decrease in TOC value from ~90 to ~43 ppm after the first cycle of emulsion separation. Due to the surface modification by electrospinning process, the wetting characteristic enables the fibers to separate oil/water emulsions effectively.

Declarations

Ethical Approval There are no ethical issues involved in this study.

Competing Interests The authors declare no competing interests.

References

1. Wu Y, Yan M, Lu J, Wang C, Zhao J, Cui J, Li C, Yan Y (2017) Facile bio-functionalized design of thermally responsive molecularly imprinted composite membrane for temperature-dependent recognition and separation applications. Chem Eng J 309:98–107
2. El-Samak AA, Ponnamma D, Hassan MK, Ammar A, Adham S, Al-Maadeed MA, Karim A (2020) Designing flexible and porous fibrous membranes for oil water separation—a review of recent developments. Polym Rev 1–46
3. Alsalhy QF, Almukhtar RS, Alani HA (2016) Oil refinery wastewater treatment by using membrane bioreactor (MBR). Arab J Sci Eng 41(7):2439–2452
4. Saadati J, Pakizeh M (2017) Separation of oil/water emulsion using a new PSf/pebax/F-MWCNT nanocomposite membrane. J Taiwan Inst Chem Eng 71:265–276
5. Park E, Barnett SM (2001) Oil/water separation using nanofiltration membrane technology. Sep Sci Technol 36(7):1527–1542
6. Chen W, Su Y, Zheng L, Wang L, Jiang Z (2009) The improved oil/water separation performance of cellulose acetate-graft-polyacrylonitrile membranes. J Membr Sci 337(1–2):98–105
7. Kim SJ, Oh BS, Yu HW, Kim LH, Kim CM, Yang ET, Shin MS, Jang A, Hwang MH, Kim IS (2015) Foulant characterization and distribution in spiral wound reverse osmosis membranes from different pressure vessels. Desalination 370:44–52
8. Obaid M, Yang E, Kang DH, Yoon MH, Kim IS (2018) Underwater superoleophobic modified polysulfone electrospun membrane with efficient antifouling for ultrafast gravitational oil-water separation. Sep Purif Technol 200:284–293
9. Lu J, Li F, Miao G, Miao X, Ren G, Wang B, Song Y, Li X, Zhu X (2021) Superhydrophilic/superoleophobic shell powder coating as a versatile platform for both oil/water and oil/oil separation. J Membr Sci 637:119624

10. Li J, Bai X, Tang X, Zha F, Feng H, Qi W (2018) Underwater superoleophobic/underoil superhydrophobic corn cob coated meshes for on-demand oil/water separation. Sep Purif Technol 195:232–237

11. Al-Anzi BS, Siang OC (2017) Recent developments of carbon based nanomaterials and membranes for oily wastewater treatment. RSC Adv 7(34):20981–20994

12. Noamani S, Niroomand S, Rastgar M, Sadrzadeh M (2019) Carbon-based polymer nanocomposite membranes for oily wastewater treatment. NPJ Clean Water 2(1):1–4

13. Yin J, Deng B (2015) Polymer-matrix nanocomposite membranes for water treatment. J Membr Sci 479:256–275

14. Hussain A, Janson A, Matar JM, Adham S (2021) Membrane distillation: recent technological developments and advancements in membrane materials. Emergent Mater 1–21

15. Lin Q, Zeng G, Yan G, Luo J, Cheng X, Zhao Z, Li H (2022) Self-cleaning photocatalytic MXene composite membrane for synergistically enhanced water treatment: oil/water separation and dyes removal. Chem Eng J 427:131668

16. Su R, Li S, Wu W, Song C, Liu G, Yu Y (2020) Recent progress in electrospun nanofibrous membranes for oil/water separation. Sep Purif Technol 117790

17. Esteves RJ, Gornick V, Alqurwani DS, Koenig-Lovejoy J, Abdelrazeq H, Khraisheh M, Forzano AV, Gad-el-Hak M, Tafreshi HV, McLeskey JT (2020) Activated carbon-doped polystyrene fibers for direct contact membrane desalination. Emergent Mater 1–8

18. Elgawady Y, Ponnamma D, Adham S, Al-Maas M, Ammar A, Alamgir K, Al-Maadeed MA, Hassan MK (2020) Mesoporous silica filled smart super oleophilic fibers of triblock copolymer nanocomposites for oil absorption applications. Emergent Mater 3(3):279–290

19. Parangusan H, Ponnamma D, Hassan MK, Adham S, Al-Maadeed MA (2019) Designing carbon nanotube-based oil absorbing membranes from gamma irradiated and electrospun polystyrene nanocomposites. Materials 12(5):709

20. Ponnamma D, Nair S, Parangusan S, K Hassan H, Adham M, Karim S, Al Ali Al-Maadeed A (2020) White graphene-cobalt oxide hybrid filler reinforced polystyrene nanofibers for selective oil absorption. Polymers 12(1):4

21. Huang T, Zhang L, Chen H, Gao C (2015) Sol–gel fabrication of a non-laminated graphene oxide membrane for oil/water separation. J Mater Chem A 3(38):19517–19524

22. Mehranbod N, Khorram M, Azizi S, Khakinezhad N (2021) Modification and superhydrophilization of electrospun polyvinylidene fluoride membrane using graphene oxide-chitosan nanostructure and performance evaluation in oil/water separation. J Environ Chem Eng 9(5):106245

23. Ngo QP, Yuan W, Wu YC, Swager TM (2023) Emulsion assembly of graphene oxide/polymer composite membranes. ACS Appl Mater Interfaces 15(17):21384–21393

24. Cui J, Zhang Y, Pan Y, Li J, Xie A, Xue C, Pan J (2023) Preparation of antifouling zwitterion PVDF-imprinted composite membranes for selective antibiotic and oil/water emulsion separation. React Funct Polym 187:105580

25. Li J, Huang S, Zhang L, Zhao H, Zhao W, Yuan C, Zhang X (2023) One-pot in-situ deposition toward fabricating superhydrophobic fiberglass membranes with composite microstructure for fast water-in-oil emulsions separation. Sep Purif Technol 313:123480

26. Zeng G, Wei K, Zhang H, Zhang J, Lin Q, Cheng X, Sengupta A, Chiao YH (2021) Ultra-high oil-water separation membrane based on two-dimensional MXene (Ti3C2Tx) by co-incorporation of halloysite nanotubes and polydopamine. Appl Clay Sci 211:106177

27. Kim KS, Lee KH, Cho K, Park CE (2002) Surface modification of polysulfone ultrafiltration membrane by oxygen plasma treatment. J Membr Sci 199(1–2):135–145

28. Pagidi A, Saranya R, Arthanareeswaran G, Ismail AF, Matsuura T (2014) Enhanced oil–water separation using polysulfone membranes modified with polymeric additives. Desalination 344:280–288

29. Rahimpour A, Madaeni SS, Taheri AH, Mansourpanah Y (2008) Coupling TiO2 nanoparticles with UV irradiation for modification of polyethersulfone ultrafiltration membranes. J Membr Sci 313(1–2):158–169

30. Pourjafar S, Rahimpour A, Jahanshahi M (2012) Synthesis and characterization of PVA/PES thin film composite nanofiltration membrane modified with TiO2 nanoparticles for better performance and surface properties. J Ind Eng Chem 18(4):1398–1405

31. Cheshomi N, Pakizeh M, Namvar-Mahboub M (2018) Preparation and characterization of TiO2/Pebax/(PSf-PES) thin film nanocomposite membrane for humic acid removal from water. Polym Adv Technol 29(4):1303–1312

32. Azuma R et al (2018) Solution synthesis of N, N-dimethylformamide-stabilized iron-oxide nanoparticles as an efficient and recyclable catalyst for alkene hydrosilylation. ChemCatChem 11:2378–2382

33. Rong F, Liu D, Zhiyong H (2018) Stability of oil-in-water emulsions by SDS compound. Pet Sci Technol 24:2157–2162

34. Rahman SS, Ur (2017) Single step growth of iron oxide nanoparticles and their use as glucose biosensor. Results in Physics 7:4451–4456

35. Schwaminger SP, Syhr C, Berensmeier S (2020) Controlled synthesis of magnetic iron oxide nanoparticles: magnetite or maghemite? Curr Comput-Aided Drug Des 10(3):214

36. De Marco C, FabricioFerrarini JS, Carli LN, Bonetto LR, Giovanela M (2014) Synthesis, characterization and application of a ferromagnetic composite in the removal of methyl violet 2B dye. Eurasia waste management symposium. 1–8

37. Theron SA, Zussman E, Yarin AL (2004) Experimental investigation of the governing parameters in the electrospinning of polymer solutions. Polymer 45(6):2017–2030

38. Deitzel JM, Kleinmeyer J, Harris DE, Tan NB (2001) The effect of processing variables on the morphology of electrospun nanofibers and textiles. Polymer 42(1):261–272

39. Yan X, Gevelber M (2010) Investigation of electrospun fiber diameter distribution and process variations. J Electrostat 68(5):458–464

40. Bodhibukkana C, Srichana T, Kaewnopparat S, Tangthong N, Bouking P, Martin GP, Suedee R (2006) Composite membrane of bacterially-derived cellulose and molecularly imprinted polymer for use as a transdermal enantioselective controlled-release system of racemic propranolol. J Control Release 113(1):43–56

41. Mehta R, Brahmbhatt H, Mukherjee M, Bhattacharya A (2017) Tuning separation behavior of tailor-made thin film poly (piperazine-amide) composite membranes for pesticides and salts from water. Desalination 404:280–290

42. Saxena M, Sharma S, Bhattacharya A (2015) Recycling of polysulfone: study properties of membranes. Int J Membr Sci Technol 2:39–46

43. Homogen M (2018) Synthesis and physicochemical properties of magnetite nanoparticles (Fe3O4) as potential solid support for homogeneous catalysts. Malays J Anal Sci 22:768–774

44. Li H, Cui Y, Wang H, Zhu Y, Wang B (2017) Preparation and application of polysulfone microcapsules containing Tung oil in self-healing and self-lubricating epoxy coating. Colloids Surf a 518:181–187

45. Ionita M, Pandele AM, Crica LE, Obreja AC (2016) Preparation and characterization of polysulfone/ammonia-functionalized

graphene oxide composite membrane material. High Perform Polym 28(2):181–188

46. Yan KK, Jiao L, Lin S, Ji X, Lu Y, Zhang L (2018) Superhydrophobic electrospun nanofiber membrane coated by carbon nanotubes network for membrane distillation. Desalination 437:26–33

47. Hammami MA, Croissant JG, Francis L, Alsaiari SK, Anjum DH, Ghaffour N, Khashab NM (2017) Engineering hydrophobic organosilica nanoparticle-doped nanofibers for enhanced and fouling resistant membrane distillation. ACS Appl Mater Interfaces 9(2):1737–1745

48. Cai Y, Chen D, Li N, Xu Q, Li H, He J, Lu J (2017) Nanofibrous metal–organic framework composite membrane for selective efficient oil/water emulsion separation. J Membr Sci 543:10–17

49. Wu M, Mu P, Li B, Wang Q, Yang Y, Li J (2020) Pine powders-coated PVDF multifunctional membrane for highly efficient switchable oil/water emulsions separation and dyes adsorption. Sep Purif Technol 248:117028

50. Chen W, Peng J, Su Y, Zheng L, Wang L, Jiang Z (2009) Separation of oil/water emulsion using Pluronic F127 modified polyethersulfone ultrafiltration membranes. Sep Purif Technol 66(3):591–597

51. Dardor D, Al-Maas M, Minier-Matar J, Janson A, Sharma R, Hassan MK, Al-Maadeed MA, Adham S (2021) Protocol for preparing synthetic solutions mimicking produced water from oil and gas operations. ACS Omega 6(10):6881–6892

52. Al-Maas M, Hussain A, Minier-Matar J, Hassan MK, Al-Maadeed MA, Alamgir K, Adham S (2022) Performance evaluation of emerging block copolymer membranes for oil-water separation. Green Technol Resil Sustain 2(1):4

53. Yang HC, Liao KJ, Huang H, Wu QY, Wan LS, Xu ZK (2014) Mussel-inspired modification of a polymer membrane for ultrahigh water permeability and oil-in-water emulsion separation. J Mater Chem A 2(26):10225–10230

54. Wang J, Hou LA, Yan K, Zhang L, Yu QJ (2018) Polydopamine nanocluster decorated electrospun nanofibrous membrane for separation of oil/water emulsions. J Membr Sci 547:156–162

55. Ebrahimi F, Nabavi SR, Omrani A (2022) Fabrication of hydrophilic special sandwich structure of PAN/GO/SiO2 electrospun membrane decorated with SiO2 nanoparticles for oil/water separation. J Water Process Eng 48:102926

56. Wang K, Zhang TC, Wei B, Chen S, Liang Y, Yuan S (2021) Durable CNTs reinforced porous electrospun superhydrophobic membrane for efficient gravity driven oil/water separation. Colloids Surf A 608:125342

57. Chen X, Zhan Y, Sun A, Feng Q, Yang W, Dong H, Chen Y, Zhang Y (2022) Anchoring the TiO2@ crumpled graphene oxide core–shell sphere onto electrospun polymer fibrous membrane for the fast separation of multi-component pollutant-oil–water emulsion. Sep Purif Technol 298:121605

58. Kou X, Han N, Zhang Y, Tian S, Li P, Wang W, Wu C, Li W, Yan X, Zhang X (2021) Fabrication of polyphenylene sulfide nanofibrous membrane via sacrificial templated-electrospinning for fast gravity-driven water-in-oil emulsion separation. Sep Purif Technol 275:119124

59. Duman O, Uğurlu H, Diker CÖ, Tunç S (2022) Fabrication of highly hydrophobic or superhydrophobic electrospun PVA and agar/PVA membrane materials for efficient and selective oil/water separation. J Environ Chem Eng 10(3):107405